Estimation of Functional Derivatives

Peter Hall[*,1], Hans-Georg Müller[**,2] and Fang Yao[***,3]

[*]Department of Mathematics and Statistics, University of Melbourne, Parkville, VIC, 3010,

Australia and Department of Statistics, University of California, Davis, CA 95616, USA

[**]Department of Statistics, University of California, Davis, CA 95616, USA

[***]Department of Statistics, University of Toronto, 100 St. George Street, Toronto, ON

M5S 3G3, Canada

January 2009

Abstract

Situations of a functional predictor paired with a scalar response are increasingly encountered in data analysis. Predictors are often appropriately modeled as square integrable smooth random functions. Imposing minimal assumptions on the nature of the functional relationship, we aim at estimating the directional derivatives and gradients of the response with respect to the predictor functions. In statistical applications and data analysis, functional derivatives provide a quantitative measure of the often intricate relationship between changes in predictor trajectories and those in scalar responses. This approach provides a natural extension of classical gradient fields in vector space and provides directions of steepest descent. We suggest a kernel-based method for the nonparametric estimation of functional derivatives that utilizes the decomposition of the random predictor functions into their eigenfunctions. These eigenfunctions define a canonical set of directions into which the gradient field is expanded. The proposed method is shown to lead to asymptotically consistent estimates of functional derivatives and is illustrated in an application to growth curves.

Key words and phrases: consistency, functional data analysis, gradient field, growth curve, Karhunen-Loève expansion, principal component, small ball probability

1. Introduction

Situations where one is given a functional predictor and a continuous scalar response are increasingly common in modern data analysis. While most studies to date have focused on functional linear models, the structural constraints imposed by these models are often undesirable. To enhance flexibility, several nonparametric functional regression approaches have been discussed. Since these models are not subject to any assumptions except smoothness, they are very widely applicable. The price one pays, of course, is that convergence will be slower when compared with functional linear models. The situation is comparable to that of extending ordinary linear regression to nonparametric regression. By abandoning restrictive assumptions, such extensions greatly enhance flexibility and breadth of applicability. Under suitable regularity assumptions, convergence of such functional nonparametric models is guaranteed for a much larger class of functional relationships and this insurance is often well worth the slower rates of convergence.

Suppose we observe a sample of i.i.d. data $(X_1, Y_1), \ldots, (X_n, Y_n)$, generated by the model

$$Y = g(X) + \epsilon, \tag{1}$$

where X is a random function in the class $L_2(\mathcal{I})$ of square-integrable functions on the interval $\mathcal{I} = [0, 1]$, g is a smooth functional from $L_2(\mathcal{I})$ to the real line, and ϵ represents an error, independent of X, with zero expected value and finite variance. In the nonparametric approach, one aims to conduct inference about g without imposing specific structure, usually that g is a linear functional. The traditional functional linear model would have $g(x) = a + \int bx$, where a is a constant and b a function, but even here the "regression parameter function" b cannot be estimated at the parametric rate $n^{-1/2}$ unless it is subject to a finite-parameter model; this model has been well investigated in the literature. Examples of such investigations include Ramsay and Dalzell (1991); Cuevas et al. (2002); Cardot et al. (2003a,b); Hall and Horowitz (2007); James and Silverman (2005); Ramsay and Silverman (2005); Yao et al. (2005b).

While the functional linear regression model has been shown to provide satisfactory fits

in various applications, it imposes a linear restriction on the regression relationship and therefore cannot adequately reflect nonlinear relations. The situation is analogous to the case of a simple linear regression model where a nonparametric regression approach often provides a much more adequate and less biased alternative approach. Likewise, there is sometimes strong empirical evidence, for example in the form of skewness of the distributions of empirical component scores, that the predictor function X is not Gaussian. The problem of estimating a nonparametric functional regression relation g in the general setting of (1) is more difficult compared to functional linear regression, and the literature is much sparser. It includes the works of Gasser et al. (1998) and Hall and Heckman (2002) on the estimation of distributions and modes in function spaces, and of Ferraty and Vieu (2003, 2004, 2006) on nonparametric regression with functional predictors. Recent developments are reviewed in Ferraty et al. (2007).

To lay the foundations for our study we introduce an orthonormal basis for $L_2(\mathcal{I})$, say $\psi_1, \psi_2, \ldots$, which in practice would generally be the basis connected to the spectrum of the covariance operator, $V(s,t) = \mathrm{cov}\{X(s), X(t)\}$:

$$V(s,t) = \sum_{j=1}^{\infty} \theta_j\, \psi_j(u)\, \psi_j(v)\,, \tag{2}$$

where the ψ_j's are the orthonormal eigenfunctions, and the θ_j's are the respective eigenvalues, of the linear operator with kernel V. The terms in (2) are ordered as $\theta_1 \geq \theta_2 \geq \ldots$. The empirical versions of the ψ_j's and θ_j's arise from a similar expansion of the standard empirical approximation $\widehat{V}$ to V,

$$\widehat{V}(s,t) = \frac{1}{n} \sum_{i=1}^{n} \{X_i(s) - \bar{X}(s)\}\, \{X_i(t) - \bar{X}(t)\} = \sum_{j=1}^{\infty} \hat{\theta}_j\, \hat{\psi}_j(s)\, \hat{\psi}_j(t)\,, \tag{3}$$

where $\bar{X} = n^{-1} \sum_i X_i$ and order is now determined by $\hat{\theta}_1 \geq \hat{\theta}_2 \geq \ldots$. The eigenvalues $\hat{\theta}_j$ vanish for $j \geq n+1$, so the functions $\hat{\psi}_{n+1}, \hat{\psi}_{n+2}, \ldots$ may be determined arbitrarily.

The centered form of X admits a Karhunen-Loève expansion,

$$X - E(X) = \sum_{j=1}^{\infty} \xi_j\, \psi_j\,, \tag{4}$$

where the principal components $\xi_j = \int_{\mathcal{I}} X \, \psi_j$ are uncorrelated and have zero means and respective variances θ_j. Their empirical counterparts are computed using $\hat{\psi}_j$ in place of ψ_j.

The paper is organized as follows. In section 2, we describe the kernel-based estimators that we consider for estimating the nonparametric regression function g in model (1) on the functional domain and for estimating functional derivatives in the directions of the eigen-functions ψ_j. Rates of convergence for kernel estimators $\hat{g}$ of the nonparametric regression function g are obtained under certain regularity assumptions on predictor processes and their spectrum (Theorems 1–3). These results then lead to the consistency property (Theorem 4) for functional derivatives. A case study concerning an application of functional derivatives to the Berkeley longitudinal growth study is the theme of section 4, followed by a compilation of the proofs in section 5.

2. Proposed Estimation Procedures

Define the Nadaraya-Watson estimator,

$$\hat{g}(x) = \frac{\sum_i Y_i \, K_i(x)}{\sum_i K_i(x)},$$

where $K_i(x) = K(\|x - X_i\|/h)$, K is a kernel function and h a bandwidth. Here $\|\cdot\|$ denotes the standard L^2 norm. Similar kernel estimators have been suggested in the literature. We refer to Ferraty and Vieu (2006) for an overview regarding these proposals and also for the previously published consistency results for the estimation of g. While the focus of this paper is on the estimation of functional derivatives in the general framework of model (1), using the spectral decomposition for predictor processes X and characterizing these processes by their eigenbasis also leads to useful and relevant results regarding the estimation of g. These results are given in Theorems 1 and 2 below, while Theorem 3 provides relevant bounds for the probability that X lies in a small ball and Theorem 4 yields the desired asymptotic consistency of the proposed functional derivative estimator defined at 7).

For simplicity we shall suppose the following (although more general conditions may be imposed).

Assumption 1. Kernel K is nonincreasing on $[0, c]$, where $c > 0$, and the support of K equals $[0, c]$.

The derivative of g at x is defined to be the linear operator g_x with the property that, for functions y and scalars δ,

$$g(x + \delta y) = g(x) + \delta \, g_x y + o(\delta)$$

as $\delta \to 0$. We may write

$$g_x = \sum_{j=1}^{\infty} \gamma_{xj} \, t_j \,, \tag{5}$$

where $\gamma_{xj} = g_x \psi_j$ is a scalar, and t_j denotes the operator that takes y to $y_j = t_j(y) = \int y \, \psi_j$. We can think of γ_{xj} as the component of g_x in the direction ψ_j.

From knowledge of the operator g_x, accessible through the components γ_{xj}, we can obtain information about functional gradients and extrema. For example, suppose $a_x^{\min} = (a_{x1}^{\min}, a_{x2}^{\min}, \ldots)$ and $a_x^{\max} = (a_{x1}^{\max}, a_{x2}^{\max}, \ldots)$ are defined as the vectors $a = (a_1, a_2, \ldots)$ that respectively minimize and maximize $|g_x a|$, where

$$g_x a = \sum_{j=1}^{\infty} \gamma_{xj} \, a_j \,, \tag{6}$$

over functions $a = \sum_j a_j \, \psi_j$ for which $\|a\| = 1$, i.e. such that $\sum_j a_j^2 = 1$. Then the function g changes fastest as we move away from x in the direction of $a_x^{\max} = \sum_j a_{xj}^{\max} \, \psi_j$, which therefore is a gradient direction. The function changes least when we move from x in the direction of $a_x^{\min} = \sum_j a_{xj}^{\min} \, \psi_j$. Extremal points are characterized by $\gamma_{xj} = 0$ for all j and their identification is of obvious interest to identify predictor functions associated with maximal or minimal responses, and also the level of these responses.

Thus, the components γ_{xj} are of intrinsic interest. As a prelude to estimating them, we introduce $Y_{i_1 i_2} = Y_{i_1} - Y_{i_2}$ and $\hat{\xi}_{i_1 i_2 j} = \int_{\mathcal{I}} (X_{i_1} - X_{i_2}) \, \hat{\psi}_j$, the latter being an empirical approximation to $\xi_{i_1 i_2 j} = \xi_{i_1 j} - \xi_{i_2 j}$, i.e. to the difference between the principal components $\xi_{ij} = \int X_i \, \psi_j$ for $i = i_1, i_2$. Define

$$Q_{i_1 i_2 j} = 1 - \frac{|\int (X_{i_1} - X_{i_2}) \, \hat{\psi}_j|^2}{\|X_{i_1} - X_{i_2}\|^2} = 1 - \frac{\hat{\xi}_{i_1 i_2 j}^2}{\|X_{i_1} - X_{i_2}\|^2} \,,$$

4

which represents the proportion of the function $X_{i_1} - X_{i_2}$ that is "not aligned in the direction of $\hat{\psi}_j$." Therefore, $Q_{i_1 i_2 j}$ will be small in cases where $X_{i_1} - X_{i_2}$ is close to being in the direction of $\hat{\psi}_j$, and will be larger in other settings. We suggest taking

$$\hat{\gamma}_{xj} = \frac{\sum \sum_{i_1,i_2}^{(j)} Y_{i_1 i_2} K(i_1, i_2, j \,|\, x)}{\sum \sum_{i_1,i_2}^{(j)} \hat{\xi}_{i_1 i_2 j} K(i_1, i_2, j \,|\, x)}. \tag{7}$$

Here, $\sum \sum_{i_1,i_2}^{(j)}$ denotes summation over pairs (i_1, i_2) such that $\hat{\xi}_{i_1 i_2 j} > 0$,

$$K(i_1, i_2, j \,|\, x) = K\left(\frac{\|x - X_{i_1}\|}{h_1}\right) K\left(\frac{\|x - X_{i_2}\|}{h_1}\right) K\left(\frac{Q_{i_1 i_2 j}}{h_2}\right), \tag{8}$$

K is a kernel function and h_1 and h_2 denote bandwidths. On the right-hand side of (8), the last factor serves to confine the estimator's attention to pairs (i_1, i_2) for which $X_{i_1} - X_{i_2}$ is close to being in the direction of $\hat{\psi}_j$, and the other two factors restrict the estimator to i_1 and i_2 such that both X_{i_1} and X_{i_2} are close to x. The estimator $\hat{\gamma}_{xj}$ uses two smoothing parameters, h_1 and h_2.

3. Theoretical Properties

3.1 Consistency and convergence rates of estimators of g

To ensure consistency we ask that the functional g be continuous at x, i.e. that for functions y and scalars δ, the following holds.

Assumption 2.

$$\sup_{y\,:\,\|y\|\leq 1} |g(x + \delta y) - g(x)| \to 0 \quad \text{as} \quad \delta \downarrow 0, \tag{9}$$

and the bandwidth h does not decrease to zero too slowly, in the sense that, with c as in Assumption 1,

$$h = h(n) \to 0 \text{ and } n\, P(\|X - x\| \leq c_1 h) \to \infty \text{ as } n \to \infty, \text{ where } c_1 = c \text{ if } K(c) > 0,$$
$$\text{and otherwise } c_1 \in (0, c). \tag{10}$$

Given $C > 0$, $x \in L_2(\mathcal{I})$ and $\alpha \in (0, 1]$, let $\mathcal{G}(C, x, \alpha)$ denote the set of functionals g such that $|g(x + \delta y) - g(x)| \leq C\,\delta^\alpha$, for all $y \in L_2(\mathcal{I})$ satisfying $\|y\| \leq 1$, and for all $0 \leq \delta \leq 1$. When deriving convergence rates we strengthen (9) by asking that g be in $\mathcal{G}(C, x, \alpha)$.

Let $\mathcal{X} = \{X_1, \ldots, X_n\}$ denote the set of explanatory variables.

Theorem 1. If Assumptions 1 and 2 hold, then $\hat{g}(x) \to g(x)$ in mean square, conditional on $\mathcal{X}$, and

$$\sup_{g \in \mathcal{G}(C,x,\alpha)} E\left[\{\hat{g}(x) - g(x)\}^2 \,\Big|\, \mathcal{X}\right] = o_p(1). \tag{11}$$

Furthermore, for all $\eta > 0$,

$$\sup_{g \in \mathcal{G}(C,x,\alpha)} P\{|\hat{g}(x) - g(x)| > \eta\} \to 0.$$

Moreover, if h is chosen to decrease to zero in such a manner that

$$h^{2\alpha} P(\|X - x\| \le c_1 h) \asymp n^{-1} \tag{12}$$

as $n \to \infty$, then for each $C > 0$ the rate of convergence of $\hat{g}(x)$ to $g(x)$ equals $O_p(h^{2\alpha})$, uniformly in $g \in \mathcal{G}(C, x, \alpha)$:

$$\sup_{g \in \mathcal{G}(C,x,\alpha)} E\left[\{\hat{g}(x) - g(x)\}^2 \,\Big|\, \mathcal{X}\right] = O_p(h^{2\alpha}), \tag{13}$$

$$\lim_{C_1 \to \infty} \limsup_{n \to \infty} \sup_{g \in \mathcal{G}(C,x,\alpha)} P\{|\hat{g}(x) - g(x)| > C_1 h^\alpha\} = 0. \tag{14}$$

To interpret (11) and (13), assume that the pairs (X_i, ϵ_i), for $1 \le i < \infty$, are all defined on the same probability space, and then put $Y_i = Y_i(g) = g(X_i) + \epsilon_i$. Write $E_g(\cdot \,|\, \mathcal{X})$ to denote expectation in the distribution of the pairs $(X_i, Y_i(g))$, conditional on $\mathcal{X}$. In section 5.1 below we shall discuss appropriateness of conditions such as (12) which relate to "small ball probabilities". Asymptotic consistency results for g and mean squared errors have been derived in Ferraty et al. (2007) under different assumptions. The convergence rate at (14) is optimal in the following sense.

Theorem 2. If the error ϵ in (1) is normally distributed, and if, for a constant $c_1 > 0$, $n P(\|X - x\| \le c_1 h) \to \infty$ and (12) holds, then for any estimator $\tilde{g}(x)$ of $g(x)$, and for $C > 0$ sufficiently large in the definition of $\mathcal{G}(C, x, \alpha)$, there exists a constant $C_1 > 0$ such that

$$\limsup_{n \to \infty} \sup_{g \in \mathcal{G}(C,x,\alpha)} P\{|\tilde{g}(x) - g(x)| > C_1 h^\alpha\} > 0.$$

According to this result, uniformity of the convergence holds over the Lipschitz class of functionals $\mathcal{G}(C, x, \alpha)$. This result applies for a fixed argument x in the domain of the predictor functions, where the functionals are evaluated. Further discussion of the bounds on $P(\|X - x\| \le u)$ as relevant for (12) is provided in Section 5.1.

3.2 Consistency of derivative estimator

We shall establish consistency of the estimator $\hat{\gamma}_{xj}$. To this end, let

$$q_{12j} = 1 - \frac{|\int (X_1 - X_2)\,\psi_j|^2}{\|X_1 - X_2\|^2}$$

denote the version of Q_{12j} when $\hat{\xi}_{i_1 i_2}$ is replaced by the quantity ξ_j that $\hat{\xi}_{i_1 i_2}$ approximates, and let $k_{i_1 i_2 j}$ denote the version of $K(i_1, i_2, j \mid x)$, defined at (8), when $Q_{i_1 i_2 j}$ there is replaced by $q_{i_1 i_2 j}$.

Assumption 3.

(a) $\sup_{t \in \mathcal{I}} E\{X(t)^4\} < \infty$;

(b) there are no ties among the eigenvalues $\theta_1, \ldots, \theta_{j+1}$;

(c) $|g(x + y) - g(x) - g_x y| = o(\|y\|)$ as $\|y\| \to 0$;

(d) the distribution of $\xi_{1j} - \xi_{2j}$ has a well-defined density in a neighborhood of the origin, not vanishing at the origin;

(e) K is supported on $[0, 1]$, nondecreasing and with a bounded derivative on the positive half-line, and $0 < K(0) < \infty$; and

(f) $h_1, h_2 \to 0$ as n increases, sufficiently slowly to ensure that $n^{1/2} \min(h_1, h_2) \to \infty$ and $(nh_1)^2 E(k_{i_1 i_2 j}) \to \infty$.

Finite variance of X guarantees that the covariance operator V, leading to the eigenfunctions ψ_j and their estimators $\hat{\psi}_j$ in section 3.1, is well defined; and finite fourth moment, stipulated by Assumption 4(a), ensures that $\|\hat{\psi}_j - \psi_j\|$ converges to zero at the standard root-n rate. This assumption is for example satisfied for Gaussian processes with smooth mean and covariance functions.

7

If we suppose in addition that X is a process with independent principal component scores $\int X \psi_j$ (or the stronger assumption that X is Gaussian) and all the eigenvalues θ_j are nonzero (we shall refer to these properties jointly as (P_1)), then Assumption 3(f) implies that $n^{-\epsilon} = O(h_j)$ for $j = 1, 2$ and for all $\epsilon > 0$ (call this property (P_2)). That is, both bandwidths are of larger order than any polynomial in n^{-1}. To see why, note that (P_1) entails $P(\|x - X\| \leq h_1) = O(h_1^{C_1})$ for all $C_1 > 0$. Also, 3(f) implies that $n h_1 P(\|x - X\| \leq C_2 h_1) \to \infty$ for some $C_2 > 0$, and this, together with (P_1), leads us to conclude that $n h^{C_1+1} \to \infty$ for all $C_1 > 0$. That result is equivalent to (P_2) for the bandwidth h_1. Property (P_1) also implies that $P(q_{12j} \leq h_2) = O(h_2^{C_1})$ for all $C_1 > 0$, and 3(f) implies that $n P(q_{12j} \leq C_2 h_2) \to \infty$ for some $C_2 > 0$, which as before leads to (P_1), this time for the second bandwidth.

Theorem 3. If Assumption 3 holds, then $\hat{\gamma}_{xj} \to \gamma_{xj}$ in probability.

Using notation (5), if $e = \sum_{j=1}^{j_0} e_j \psi_j$ with $\sum_j e_j^2 = 1$ and $j_0 < \infty$, the functional directional derivative in direction e at x is $g_x e = \sum_j e_j \gamma_{xj}$; see also (6), where e is obtained by choosing $a_j = e_j$, $1 \leq j \leq j_0$, $a_j = 0$, $j > j_0$. If Assumption 3 holds for all $j \leq j_0$, it is an immediate consequence of Theorem 3 that the estimated functional derivative $\hat{g}_x e = \sum_j e_j \hat{\gamma}_{xj}$ at x in direction e is consistent, i.e., satisfies $\hat{g}_x e \to g_x e$ in probability. As this holds uniformly over all direction vectors e, the functional gradient field for directions anchored in the span of $\{\psi_1, \ldots, \psi_{j_0}\}$ can be estimated consistently.

If we take the operator $\hat{g}_x$, defined by $\hat{g}_x a = \sum_{j \leq r} \hat{\gamma}_{xj} a_j$ (where $r \geq 1$ is an integer and $a = \sum_j a_j \psi_j$ is function), to be an empirical approximation to g_x, the operator given by $g_x a = \sum_j \gamma_{xj} a_j$, if the conditions in Assumption 3 hold for each j, and in addition $\sum_j \gamma_{xj}^2 < \infty$, then there exists a (generally unknown) deterministic sequence $r = r(n, x)$ with the following properties: $r(n, x) \to \infty$ as $n \to \infty$; whenever $\|a\| < \infty$, $\hat{g}_x a - g_x a \to 0$ in probability; and moreover, $\hat{g}_x \to g_x$ in norm as $n \to \infty$, where the convergence is again in probability. An explicit construction of such a sequence $r(n, x)$, and thus of an explicit estimate of the derivative operator with these properties, would require further results regarding the convergence rates for varying j in Theorem 3, and remains an open problem.

4. Application of functional derivative estimation to growth data

The analysis of growth data has a long tradition in statistics. It played a pioneering role in the development of functional data analysis, as evidenced by the studies of Rao (1958); Gasser et al. (1984); Kneip and Gasser (1992); Ramsay and Li (1998) and Gervini and Gasser (2005) and remains an active field of statistical research to this day.

We explore the relationship between adult height, measured at age 18 (scalar response), and the growth rate function observed to age 10 (functional predictor), for 39 boys. Of interest is the following question: How do shape changes in the prepubertal growth velocity curve relate to changes in adult height? Which changes in the shape of a prepubertal growth velocity curve of an individual will lead to the largest adult height gain for an individual? These and similar questions can be addressed by obtaining the functional gradient of the regression of adult height versus the prepubertal growth velocity trajectory. Such analyses are expected to provide us with better understanding of the intricate dynamics and regulatory processes of human growth. Functional differentiation provides an excellent vehicle for studying the effects of localized growth velocity changes during various stages of prepubertal growth on adult height.

For this exploration, we use growth data for 39 boys from the Berkeley longitudinal growth study (Tuddenham and Snyder, 1954), where we include only measurements obtained up to age 10 for the growth velocity predictor processes. The 15 time points before age 10 at which height measurements are available for each boy in the Berkeley study correspond to ages $\{1, 1.25, 1.5, 1.75, 2, 3, 4, 5, 6, 7, 8, 8.5, 9, 9.5, 10\}$, denoted by $\{s_j\}_{j=1,\ldots,15}$. Raw growth rates were calculated as first order difference quotients $X_{ij} = (h_{i,j+1} - h_{ij})/(t_{j+1} - t_j)$, where h_{ij} are the observed heights at times s_j for the ith boy, and $t_j = (s_j + s_{j+1})/2$, $i = 1, \ldots, 39$, $j = 1, \ldots, 14$. These raw data form the input for the computation of the functional decomposition of the predictor processes into mean function, eigenfunctions and functional principal component scores. To obtain this decomposition, we used an implementation of the functional spectral methods described in Yao et al. (2003) and Yao et al. (2005a).

Applying a BIC type criterion based on marginal pseudo-likelihood to choose the number of components in the eigenrepresentation, three components were selected. The resulting smooth estimates of fitted individual and mean growth velocity curves are shown in Figure 1. The first three components explain 99.5% of the total variation (78.9%, 17% and 3.6%, respectively), and the corresponding estimated eigenfunctions are displayed in the left panel of Figure 2. The first eigenfunction corresponds to a rapid initial decline in growth velocity, followed by a relatively flat increase with onset around age 5 towards the right end of the considered age range, while the second eigenfunction contains a sign change and provides a contrast between growth rates after age 2 and those before age 2. The third eigenfunction describes a midgrowth spurt around ages 6–7, coupled with an especially rapid decline in growth rate before age 3.

To visualize the estimated functional derivatives, a derivative scores plot as shown in the right panel of Figure 2 is of interest. The coefficient estimates for the first two eigendirections are plotted, i.e., the points $(\gamma_{X_i,1}, \gamma_{X_i,2})$ (defined at (5)), evaluated at each of the 39 predictor functions X_i. This figure thus represents the canonical functional gradient vectors at the observed data points, truncated at the first two components. These gradient vectors are seen to vary quite a bit across subjects, with a few extreme values present in the derivative corresponding to the first eigendirection.

The gradients are generally positive in the direction of the first eigenfunction and negative in the direction of the second. Their interpretation is relative to the shape of the eigenfunctions, including the selected sign for the eigenfunctions (as the sign of the eigenfunctions is arbitrary). If the gradient is positive in the direction of a particular eigenfunction ψ_j, it means that adult height tends to increase as the corresponding functional principal component score ξ_j increases. So in order to interpret the gradients in the right panel of Figure 2, one needs to study the shapes of the corresponding eigenfunctions as depicted in the left panel. When observing the shapes of first and second eigenfunction in the left panel of Figure 2, adult height is seen to increase most if the growth velocities towards the right end of the

domain of the growth rate predictor curves are larger, a result that is in line with what one would expect.

Using the first K components, we define functions $g_i^*(t) = \sum_{j=1}^{K} \gamma_{X_i,j} \psi_j(t)$ for each subject i. Then for any test function $z(t) = \sum_{j=1}^{K} z_j \psi_j(t)$ with $\|z\| = 1$ one has $\int g_i^*(t) z(t) \, dt = \sum_{j=1}^{K} \gamma_{X_i,j} z_j$ so that the functional directional derivative at X_i in direction z is obtained through an inner product of z with g_i^*. We therefore refer to g_i^* as the *derivative generating function* at X_i. In the application to growth curves, we choose $K = 3$ and this function can be interpreted as a subject-specific weight function, whose inner product with a test function z provides the gradient of adult height when moving from the trajectory X_i in the direction indicated by z. It is straightforward to obtain estimates

$$\hat{g}_i^*(t) = \sum_{j=1}^{K} \hat{\gamma}_{X_i,j} \hat{\psi}_j(t) \tag{15}$$

of these derivative generating functions by plugging in estimates for $\gamma_{X_i,j}$ and $\psi_j(t)$ as obtained in (3) and (7).

Estimated derivative generating functions $\hat{g}_i^*$ for $K = 3$ are depicted in Figure 3 for all 39 trajectories X_i in the sample. These empirical derivative generating functions are found to be relatively homogeneous. Estimated functional directional derivatives in any specific direction of interest are then easily obtained. We find that gradients are largest in directions $z = g_i^*/\|g_i^*\|$, i.e., in directions that are parallel to the derivative generating functions g_i^*. This means that largest increases in adult height are obtained in the presence of increased growth velocity around 2-4 years and past 8 years, while growth velocity increases between 5-7 years have only a relatively small effect.

It is of interest to associate the behavior of the derivative operators with features of the corresponding predictor trajectories. The predictor trajectories X_i for which the derivative coefficients $\gamma_{X_i,j}$ have the largest and smallest absolute values in each of the first three eigendirections (for $j = 1, 2, 3$) are depicted in the upper panels of Figure 4. The lower panels show the corresponding derivative generating functions. One finds that the functional gradients of growth velocity curves that contain time periods of relatively small growth velocity are such

11

that increased growth velocity in these time periods is associated with the largest increases in subsequent adult height (dashed curves in left and middle panel, dotted curve in right panel), as does slowing of above-normal high post-partum growth velocities (dashed curve in right panel).

A systematic visualization of the connection of predictor functions and the gradient field, as represented by the derivative generating functions, is obtained by considering families of predictor trajectories $X(t; \alpha_j) = \hat{\mu}(t) + \alpha_j \hat{\psi}_j(t)$ that move away from the mean growth velocity trajectory in the direction of a specific eigenfunction, while the other eigenfunctions are ignored, as shown in the upper panels of Figure 5 for the first three eigenfunctions. The corresponding derivative generating functions are in the lower panels. This visually confirms that adult height gains are associated with increased growth velocities in those areas where a subject's velocities are relatively low, especially towards the right end of the domain of the velocity predictor curves.

As the sample size in this example is relatively small, it is clear that caution needs to be exercised in the interpretation of the results of this data analysis. The results presented here follow the spirit of exploratory data analysis. We find that the concept of functional derivatives can lead to new insights when analyzing functional data which extend beyond those available when using established functional methods. Many practical and theoretical issues require further study. These include for example choice of window widths and the estimation of functional derivatives for data which are irregularly or sparsely measured.

5. Additional results and proofs

5.1 Bounds on $P(\|X - x\| \leq u)$

Reflecting the infinite-dimensional nature of functional-data regression, the rate of convergence of the "small ball probabilities" $P(\|X - x\| \leq u)$ to zero as $u \to 0$ is generally quite rapid, in fact faster than any polynomial in u. See (19) below. In consequence, the convergence rate of $\hat{g}(x)$ to $g(x)$ can be particularly slow. Indeed, unless the Karhunen-Loève

expansion of X is actually finite-dimensional, the rate of convergence evidenced by (14) is slower than the inverse of any polynomial in n.

The fastest rates of convergence arise when the distribution of X is closest to being finite-dimensional, for example when the Karhunen-Loève expansion of X can be written as $X = \sum_j \xi_j \psi_j$, where $\text{var}(\xi_j) = \theta_j$ and the eigenvalues θ_j, $j \geq 1$, decrease to zero exponentially, rather than polynomially, fast as j increases, where the ξ_j are uncorrelated. Therefore we shall focus primarily on this case and require

Assumption 4. For constants $B, \beta > 0$,

$$\log \theta_j = -B\, j^\beta + o(j^\beta) \text{ as } j \to \infty, \tag{16}$$

and the random variables $\eta_j = \xi_j / \theta_j^{1/2}$ are independent and identically distributed as η, the distribution of which satisfies

$$B_1 \, u^b \leq P(|\eta| \leq u) \leq B_2 \, u^b \text{ for all sufficiently small } u > 0, \text{ and}$$

$$P(|\eta| > u) \leq B_3 \, (1+u)^{-B_4} \text{ for all } u > 0, \text{ where } B_1, \ldots, B_4, b > 0. \tag{17}$$

Take $x = 0$, the zero function, and, with b, B and β as in (16) and (17), define

$$\pi(u) = \exp\left\{ -\frac{b\beta}{\beta + 1} \left(\frac{2}{B}\right)^{1/\beta} |\log u|^{(\beta+1)/\beta} \right\}. \tag{18}$$

Theorem 4. If (16) and (17) hold, then, with $\pi(u)$ given by (18),

$$P(\|X\| \leq u) = \pi(u)^{1+o(1)} \text{ as } u \downarrow 0. \tag{19}$$

Combining Theorems 1 and 3 we deduce that if the eigenvalues θ_j decrease as indicated at (16), if the principal components ξ_j have the distributional properties at (17), and if the bandwidth h is chosen so that (12) holds, then the kernel estimator $\hat{g}(x)$ converges to $g(x)$ at the mean-square rate of

$$h^{2\alpha} = \exp(-2\alpha |\log h|)$$
$$= \exp\left[-\{1+o(1)\} 2\alpha \left(\frac{\beta+1}{b\beta}\right)^{\beta/(\beta+1)} \left(\frac{B}{2}\right)^{1/(\beta+1)} (\log n)^{\beta/(\beta+1)} \right].$$

13

For each fixed β, this quantity decreases to zero more slowly than any power of n^{-1}, although the rate of decrease increases as β increases. A typical example where conditions (16) and (17) are satisfied is that of a process where $\theta_j = \exp(-B\,j^\beta)$, where the distribution of η in Assumption 4 has a bounded, nonzero density in a neighborhood of the origin, and where $\{\phi_j\}$ is the standard Fourier series. In this case one finds that $\beta = b = 1$ and $\pi(u) = \exp\{-c(\log u)^{(\beta+1)/\beta}\} = u^{-c(\log u)^{1/\beta}}$ for some $c > 0$, corresponding to faster than polynomial convergence towards 0. Of course, the condition on the distribution of η is satisfied if the process X is Gaussian.

Theorem 4 establishes that, in the case $x = 0$, the probability $P(\|X - x\| \leq u)$ typically does not vanish, even for very small u; and, in this context, (19) gives a concise account of the size of the probability. If we take $x = 0$ and replace X by $X_1 - X_2$, for which the calculations leading to (19) are identical in all essential respects to those leading to (19), then we obtain a formula for the average value of $P(\|X_1 - x\| \leq u)$ over all realizations x of X_2. Therefore (19) provides substantially more than just the value of the probability when $x = 0$. The case of fixed but nonzero x, where $x = \sum_j \theta_j^{1/2}\, x_j$ and the x_j's are uniformly bounded, can be treated with related arguments, and also the setting where the x_j's are unbounded, although it needs more detailed arguments.

If θ_j decreases to zero at a polynomial rate, rather than at the exponential rate stipulated by (16), then the probability $P(\|X - x\| \leq u)$ decreases to zero at rate $\exp(-C_1\,u^{-C_2})$ as u decreases to 0, rather than at the rate $\exp(-C_1\,|\log u|^{C_2})$ indicated by Theorem 3 for constants $C_1, C_2 > 0$. Very accurate results of this type, in the case where $x = 0$, are given by Gao et al. (2003), who also provide additional relevant references. It is noteworthy that these results also pertain to non-Gaussian processes, while early results along these lines for Gaussian processes can be found in Anderson and Darling (1952). Decay rates of the closely related type $u^{C_3} \exp(-C_1\,u^{-C_2})$ for $C_3 > 0$ were featured in Ferraty et al. (2007), among several other rates that are primarily associated with finite-dimensional processes.

We conclude from this discussion that the decay rates of the small ball probabilities are

intrinsically linked to the decay rates of the eigenvalues of the underlying process. The fast decay rates associated with polynomially converging eigenvalues mean that this case is not particularly desirable from a statistical point of view.

5.2 Proof of Theorem 1

Let σ^2 denote the variance of the error ϵ in (1). Set $N_j = \sum_i K_i(x)^j$ for $j = 1, 2$, and note that $N_2 \leq K(0) N_1$, as $K(\cdot)$ is non-increasing and compactly supported on $[0, c]$. Therefore,

$$
\begin{aligned}
E\Big[\{\hat{g}(x) - g(x)\}^2 \,\Big|\, \mathcal{X}\Big] &= \Big[E\{\hat{g}(x)|\mathcal{X}\} - g(x)\Big]^2 + \mathrm{var}(\hat{g}(x)|\mathcal{X}) \\
&\leq \max_{i=1,\ldots,n} |g(X_i) - g(x)| I(\|X_i - x\| \leq ch) + \frac{\sigma^2 \sum_i K_i^2(x)}{\{\sum_i K_i(x)\}^2} \\
&\leq \sup_{y \,:\, \|y\| \leq ch} |g(x) - g(x+y)|^2 + \frac{\sigma^2 K(0)}{N_1} .
\end{aligned}
\tag{20}
$$

Continuity of g at x, i.e. (9), implies that the first term on the right-hand side of (20) converges to zero. Note that $K_i(x) \geq K_i(x) I(\|X_i - x\| \leq c_1 h) \geq K(c_1) I(\|X_i - x\| \leq c_1 h)$, where c_1 is as in (A2). Then (10) entails $N_1^{-1} \to 0$ with probability 1, and by monotone convergence $E(N_i^{-1}) \to 0$. Together with (20), these properties imply the first part of the theorem. The second part, comprising (13) and (14), is obtained on noting that (20) entails,

$$
\begin{aligned}
\sup_{g \in \mathcal{G}(C, x, \alpha)} E\Big[\{\hat{g}(x) - g(x)\}^2 \,\Big|\, \mathcal{X}\Big] &\leq C^2 (ch)^{2\alpha} + \frac{\sigma^2 K(0)}{N_1} \\
&\leq C^2 (ch)^{2\alpha} + \frac{\sigma^2 K(0) \{1 + o_p(1)\}}{K(c_1) \, n \, P(\|X - x\| \leq c_1 h)} ,
\end{aligned}
$$

and $E(N_1^{-1}) \leq E[\{\sum_i I(\|X_i - x\| \leq c_1 h)\}^{-1}] \asymp \{nP(\|X - x\| \leq c_1 h)\}^{-1}$.

5.3 Proof of Theorem 2

Without loss of generality, $x = 0$. Let f denote a function defined on the real line, with a derivative bounded in absolute value by B_1, say, supported only within the interval $[-B_2, B_2]$, and not vanishing everywhere. Then f itself must be uniformly bounded, by B_3 say. Define $g_1 \equiv 0$ and $g_2(y) = h^\alpha f(\|y\|/h)$. If $\|y\| \leq h$ then, since $0 < \alpha \leq 1$,

$$
|g_2(y) - g_2(0)| = h^\alpha |f(\|y\|/h) - f(0)| \leq h^\alpha B_1 \|y\|/h \leq h^\alpha B_1 (\|y\|/h)^\alpha = B_1 \|y\|^\alpha ,
$$

15

while if $\|y\| > h$,

$$|g_2(y) - g_2(0)| \leq 2\, h^\alpha\, B_3 \leq 2\, B_3\, \|y\|^\alpha\,.$$

Therefore, $g_2 \in \mathcal{G}(C, 0, \alpha)$ provided $\max(B_1, 2B_3) \leq C$.

The theorem will follow if we show that, in a classification problem where we observe n data generated as at (1), with the errors distributed as Normal $N(0,1)$ and $g = g_1$ or g_2, with prior probability $\frac{1}{2}$ on either of these choices, the likelihood-ratio rule fails, in the limit as $n \to \infty$, to discriminate between g_1 and g_2. That is, with $Y_i = \epsilon_i$ (the result of taking $g = g_1$ in the model), and with ρ defined by

$$\rho = \frac{\prod_i \exp[-\frac{1}{2}\,\{Y_i - g_1(X_i)\}^2]}{\prod_i \exp[-\frac{1}{2}\,\{Y_i - g_2(X_i)\}^2]}\,,$$

we should show that

$$P(\rho > 1) \text{ is bounded below } 1 \text{ as } n \to \infty\,. \tag{21}$$

Now,

$$2 \log \rho = \sum_{i=1}^{n} \left\{ g_2(X_i)^2 - 2\, \epsilon_i\, g_2(X_i) \right\},$$

which, conditional on $\mathcal{X}$, is normally distributed with mean $s_n^2 = \sum_i g_2(X_i)^2$ and variance $4\, s_n^2$. Therefore, (21) holds if and only if

$$\lim_{B \to \infty}\, \limsup_{n \to \infty}\, P\big(s_n^2 > B\big) = 0\,, \tag{22}$$

and so we can complete the proof of Theorem 2 by deriving (22).

If we choose the radius B_2 of the support of f so that $0 < B \leq c_1$, then $|g_2(x)| \leq B_3\, h^\alpha\, I(\|x\| \leq c_1 h)$, in which case

$$s_n^2 \leq B_3^2\, h^{2\alpha} \sum_{i=1}^{n} I(\|X_i\| \leq c_1 h)\,. \tag{23}$$

Since, by assumption, $n\, P(\|X\| \leq c_1 h) \to \infty$, then

$$\frac{\sum_i I(\|X_i\| \leq c_1 h)}{n\, P(\|X\| \leq c_1 h)} \to 1$$

in probability. This property, (12) and (23) together imply (22).

5.4 Proof of Theorem 3

Write simply $K_{i_1 i_2 j}$ for $K(i_1, i_2, j \mid x)$. Assumption 3(e) implies that

$$K_{i_1 i_2 j} = 0 \text{ unless each of the following holds: } \|X_{i_1} - x\| \leq h_1,$$

$$\|X_{i_2} - x\| \leq h_1 \text{ and } Q_{i_1 i_2} \leq h_2. \tag{24}$$

Given $\delta > 0$, let $s(\delta)$ equal the supremum of $|g(x + y) - g(x) - g_x y|$ over functions y with $\|y\| \leq \delta$. Then, by Assumption 3(c),

$$\delta^{-1} s(\delta) \to 0 \quad \text{as} \quad \delta \downarrow 0. \tag{25}$$

Write $\mathcal{E}_{i_1 i_2}$ for the event that $\|X_{i_k} - x\| \leq h_1$ for $k = 1, 2$. If $\mathcal{E}_{i_1 i_2}$ holds,

$$\left| g(X_{i_1}) - g(X_{i_2}) - g_x(X_{i_1} - X_{i_2}) \right| \leq 2\, s(h_1).$$

Therefore, defining $\epsilon_{i_1 i_2} = \epsilon_{i_1} - \epsilon_{i_2}$ and assuming $\mathcal{E}_{i_1 i_2}$,

$$\left| Y_{i_1} - Y_{i_2} - \{ g_x(X_{i_1} - X_{i_2}) + \epsilon_{i_1 i_2} \} \right| \leq 2\, s(h_1).$$

Hence, defining $\xi_{i_1 i_2 j} = \xi_{i_1 j} - \xi_{i_2 j}$, noting that $g_x(X_{i_1} - X_{i_2}) = \sum_k \xi_{i_1 i_2 k}\, \gamma_{xk}$, and using (24), we have,

$$\left| \sum\sum_{i_1, i_2}^{(j)} (Y_{i_1} - Y_{i_2})\, K_{i_1 i_2 j} \right.$$
$$\left. - \left(\sum\sum_{i_1, i_2}^{(j)} K_{i_1 i_2 j} \sum_{k=1}^{\infty} \xi_{i_1 i_2 k}\, \gamma_{xk} + \sum\sum_{i_1, i_2}^{(j)} \epsilon_{i_1 i_2}\, K_{i_1 i_2 j} \right) \right|$$
$$\leq 2\, s(h_1) \sum\sum_{i_1, i_2}^{(j)} K_{i_1 i_2 j}. \tag{26}$$

Now,

$$\left| \hat{\xi}_{i_1 i_2 j} - \xi_{i_1 i_2 j} \right| = \left| \int (X_{i_1} - X_{i_2}) (\hat{\psi}_j - \psi_j) \right|$$
$$\leq \|X_{i_1} - X_{i_2}\|\, \|\hat{\psi}_j - \psi_j\| \leq 2h_1\, \|\hat{\psi}_j - \psi_j\|, \tag{27}$$

where the last inequality holds under the assumption that the event $\mathcal{E}_{i_1 i_2}$ obtains. Combining (24), (26) and (27) we deduce that

$$\left| \sum\sum_{i_1, i_2}^{(j)} (Y_{i_1} - Y_{i_2})\, K_{i_1 i_2 j} - \left(\gamma_{xj} \sum\sum_{i_1, i_2}^{(j)} \hat{\xi}_{i_1 i_2 j}\, K_{i_1 i_2 j} \right. \right.$$

17

$$+ \sum\sum_{i_1,i_2}^{(j)} K_{i_1 i_2 j} \sum_{k\,:\,k\neq j} \xi_{i_1 i_2 k}\,\gamma_{xk} + \sum\sum_{i_1,i_2}^{(j)} \epsilon_{i_1 i_2}\, K_{i_1 i_2 j} \Bigg) \Bigg|$$

$$\leq\; 2\left\{ s(h_1) + |\gamma_{xj}|\, h_1\, \|\hat{\psi}_j - \psi_j\| \right\} \sum\sum_{i_1,i_2}^{(j)} K_{i_1 i_2 j}\,. \qquad (28)$$

Note too that

$$\left| \sum\sum_{i_1,i_2}^{(j)} K_{i_1 i_2 j} \sum_{k\,:\,k\neq j} \xi_{i_1 i_2 k}\,\gamma_{xk} \right| = \left| \sum\sum_{i_1,i_2}^{(j)} K_{i_1 i_2 j} \sum_{k\,:\,k\neq j} \gamma_{xk} \int (X_{i_1} - X_{i_2})\,\psi_k \right|$$

$$\leq\; \sum\sum_{i_1,i_2}^{(j)} K_{i_1 i_2 j} \left(\sum_{k\,:\,k\neq j} \gamma_{xk}^2 \right)^{1/2} \left[\sum_{k\,:\,k\neq j} \left\{ \int (X_{i_1} - X_{i_2})\,\psi_k \right\}^2 \right]^{1/2}$$

$$\leq\; \|g_x\| \sum\sum_{i_1,i_2}^{(j)} K_{i_1 i_2 j} \left[\|X_{i_1} - X_{i_2}\|^2 - \left\{ \int (X_{i_1} - X_{i_2})\,\psi_j \right\}^2 \right]^{1/2}$$

$$\leq\; \|g_x\| \sum\sum_{i_1,i_2}^{(j)} K_{i_1 i_2 j} \Bigg[\|X_{i_1} - X_{i_2}\|^2 - \left\{ \int (X_{i_1} - X_{i_2})\,\hat{\psi}_j \right\}^2$$

$$+ 8\,\|\hat{\psi}_j - \psi_j\|\,\|X_{i_1} - X_{i_2}\|^2 \Bigg]^{1/2}$$

$$\leq\; 2\,\|g_x\|\, h_1 \sum\sum_{i_1,i_2}^{(j)} K_{i_1 i_2 j} \left(Q_{i_1 i_2 j} + 8\,\|\hat{\psi}_j - \psi_j\| \right)^{1/2}$$

$$\leq\; 2\,\|g_x\|\, h_1\, (h_2 + 8\,\|\hat{\psi}_j - \psi_j\|)^{1/2} \sum\sum_{i_1,i_2}^{(j)} K_{i_1 i_2 j}\,. \qquad (29)$$

To obtain the third-last inequality in (29) we used the fact that, with $a = |\int (X_{i_1} - X_{i_2})\,\psi_j|$, $b = |\int (X_{i_1} - X_{i_2})\,\hat{\psi}_j|$ and

$$c = \|X_{i_1} - X_{i_2}\|\,\|\hat{\psi}_j - \psi_j\| \leq 2\,\|X_{i_1} - X_{i_2}\| \leq 4h_1\,, \qquad (30)$$

where (in each of (30) and in (31) below) the last inequality is correct provided $\mathcal{E}_{i_1 i_2}$ holds, we have used the fact that $|a - b| \leq c$ and $|a| \leq \|X_{i_1} - X_{i_2}\|$ imply that

$$\left| a^2 - b^2 \right| \leq c\,(2a + c) \leq 4\,\|\hat{\psi}_j - \psi_j\|\,\|X_{i_1} - X_{i_2}\|^2 \leq 8\,\|\hat{\psi}_j - \psi_j\|\, h_1^2\,. \qquad (31)$$

To obtain the last inequality in (29) we used (24) and the fact that $Q_{i_1 i_2 j} \leq h_2$ if $K_{i_1 i_2 j} \neq 0$.

Combining (28) and (29) we find that

$$\left| \sum\sum_{i_1,i_2}^{(j)} (Y_{i_1} - Y_{i_2})\, K_{i_1 i_2 j} - \left(\gamma_{xj} \sum\sum_{i_1,i_2}^{(j)} \hat{\xi}_{i_1 i_2 j}\, K_{i_1 i_2 j} + \sum\sum_{i_1,i_2}^{(j)} \epsilon_{i_1 i_2}\, K_{i_1 i_2 j} \right) \right|$$

$$\leq\; 2\,h_1 \left\{ h_1^{-1}\, s(h_1) + |\gamma_{xj}|\,\|\hat{\psi}_j - \psi_j\| \right.$$

18

$$+\|g_x\|\,(h_2 + 8\,\|\hat{\psi}_j - \psi_j\|)^{1/2}\Big\} \sum\sum\nolimits^{(j)}_{i_1,i_2} K_{i_1 i_2 j}\,. \tag{32}$$

Result (32) controls the numerator in the definition of $\hat{\gamma}_{xj}$ at (7). To control the denominator there, use (27) to show that

$$\begin{aligned}
\sum\sum\nolimits^{(j)}_{i_1,i_2} \hat{\xi}_{i_1 i_2 j}\, K_{i_1 i_2 j} &\geq \sum\sum\nolimits^{(j)}_{i_1,i_2} \max\big(0\,,\, \xi_{i_1 j} - \xi_{i_2 j} - 2h_1\,\|\hat{\psi}_j - \psi_j\|\big)\, K_{i_1 i_2 j} \\
&\geq \sum\sum\nolimits^{(j)}_{i_1,i_2} \max(0\,,\, \xi_{i_1 j} - \xi_{i_2 j})\, K_{i_1 i_2 j} \\
&\quad - 2h_1\,\|\hat{\psi}_j - \psi_j\| \sum\sum\nolimits^{(j)}_{i_1,i_2} K_{i_1 i_2 j}\,.
\end{aligned} \tag{33}$$

(Recall that $\sum\sum^{(j)}_{i_1,i_2}$ denotes summation over (i_1,i_2) such that $\hat{\xi}_{i_1 i_2 j} > 0$.) Using Assumption 4(d), (e) and (f) it can be proved that, for a constant $B > 0$,

$$\sum\sum\nolimits^{(j)}_{i_1,i_2} \max(0\,,\, \xi_{i_1 j} - \xi_{i_2 j})\, K_{i_1 i_2 j} \geq \{1 + o_p(1)\}\, B\, h_1 \sum\sum\nolimits^{(j)}_{i_1,i_2} K_{i_1 i_2 j}\,. \tag{34}$$

(Note that, by Assumption 3(f), $n^{-1/2}/\min(h_1,h_2) \to 0$.) From Assumption 3(a) and (b) it follows that

$$\|\hat{\psi}_j - \psi_j\| = O_p\big(n^{-1/2}\big)\,. \tag{35}$$

Together, (33)–(35) imply that

$$\sum\sum\nolimits^{(j)}_{i_1,i_2} \hat{\xi}_{i_1 i_2 j}\, K_{i_1 i_2 j} \geq \{1 + o_p(1)\}\, B\, h_1 \sum\sum\nolimits^{(j)}_{i_1,i_2} K_{i_1 i_2 j}\,, \tag{36}$$

for the same constant B as in (34). This result controls the denominator at (7).

From (7), (25), (32) and (36) we deduce that

$$\hat{\gamma}_{xj} = \gamma_{xj} + O_p\left(\frac{\sum\sum^{(j)}_{i_1,i_2} \epsilon_{i_1 i_2}\, K_{i_1 i_2 j}}{h_1 \sum\sum^{(j)}_{i_1,i_2} K_{i_1 i_2 j}}\right) + o_p(1)\,. \tag{37}$$

The variance of the ratio on the right-hand side of (37), conditional on the explanatory variables X_i, equals

$$O_p\left\{\left(h_1^2 \sum\sum\nolimits^{(j)}_{i_1,i_2} K_{i_1 i_2 j}\right)^{-1}\right\} = O_p\left[\{(nh_1)^2\, E(k_{i_1 i_2 j})\}^{-1}\right] = o_p(1)\,,$$

where to obtain the last identity we used Assumption 3(f). Therefore (37) implies that $\hat{\gamma}_{xj} = \gamma_{xj} + o_p(1)$, which proves Theorem 3.

5.5 Proof of Theorem 4

Observe that, for each $t \in (0, 1)$ and with $D_t = (\sum_j \theta_j^{1-t})^{-1}$,

$$P(\|X\| \leq u) = P\left(\sum_{j=1}^{\infty} \theta_j \, \eta_j^2 \leq u^2 \right) \begin{cases} \leq \prod_{j=1}^{\infty} P(\theta_j \, \eta_j^2 \leq u^2) \\ \\ \geq \prod_{j=1}^{\infty} P(\theta_j^t \, \eta_j^2 \leq D_t \, u^2) , \end{cases} \tag{38}$$

where to obtain the lower bound we used the property,

$$P\left(\sum_{j=1}^{\infty} \theta_j \, \eta_j^2 \leq u^2 \right) = P\left\{ \sum_{j=1}^{\infty} \theta_j^{1-t} \left(\theta_j^t \, \eta_j^2 - D_t \, u^2 \right) \leq 0 \right\}$$

$$\geq P\left(\theta_j^t \, \eta_j^2 \leq D_t \, u^2 \text{ for each } j \right) .$$

Define $J = J(u)$ to be the largest integer such that $u/\theta_j^{1/2} \leq \zeta$, where ζ is chosen so small that $B_1 \, u^b \leq P(|\eta| \leq u) \leq B_2 \, u^b$ for $0 \leq u \leq \zeta$. Then,

$$\prod_{j=1}^{\infty} P(\theta_j \, \eta_j^2 \leq u^2) \leq \prod_{j=1}^{J} P(|\eta| \leq u \, \theta_j^{-1/2})$$

$$= u^{bJ} \, \exp\left\{ \tfrac{1}{2} \, bB \sum_{j=1}^{J} j^\beta + o(J^{\beta+1}) \right\}$$

$$= \exp\left\{ -\frac{bB\beta}{2(\beta+1)} \, J^{\beta+1} + o(J^{\beta+1}) \right\} = \pi(u)^{1+o(1)}, \tag{39}$$

as $u \downarrow 0$, where π is defined at (18).

Redefine J to be the largest integer such that $D_t^{1/2} u/\theta_j^{t/2} \leq \zeta$. Then, using the argument leading to (39) we may show that

$$\prod_{j=1}^{J} P(\theta_j^t \, \eta_j^2 \leq D_t \, u^2) = \exp\left\{ -\frac{b\beta}{\beta+1} \left(\frac{2}{Bt} \right)^{1/\beta} |\log u|^{(\beta+1)/\beta} + o(|\log u|^{(\beta+1)/\beta}) \right\}$$

$$= \pi(u)^{t^{-1/\beta}+o(1)} \tag{40}$$

Also, for $j \geq J + 1$,

$$\pi_j \equiv P(\theta_j^t \, \eta_j^2 > D_t \, u^2) \leq B_3 \left\{ 1 + \left(D_t^{1/2} \, u/\theta_j^{t/2} \right) \right\}^{-B_4} . \tag{41}$$

Note too that, for a constant $B_5 = B_5(t) \in (0, 1)$ we have $\pi_j \in (0, B_5)$ for $j \geq J + 1$, and

$$1 - \pi_j = \exp\left(-\sum_{k=1}^{\infty} \frac{\pi_j^k}{k} \right) \geq \exp(-B_6 \, \pi_j) ,$$

20

from which it follows that

$$\prod_{j=J+1}^{\infty} (1 - \pi_j) \geq \exp\left(- B_6 \sum_{j=J+1}^{\infty} \pi_j \right) \geq \exp\left\{ - B_7 \sum_{j=J+1}^{\infty} \left(\theta_j^{t/2} / u \right)^{B_4} \right\},$$

which is of smaller order than the right-hand side of (40). Combining this result with (40), and noting that $t \in (0, 1)$, on the right-hand side of (40), can be taken arbitrarily close to 1, we deduce that as $u \downarrow 0$,

$$\prod_{j=1}^{\infty} P\left(\theta_j^t \, \eta_j^2 \leq D_t \, u^2 \right) = \pi(u)^{1+o(1)} . \tag{42}$$

Together, (38), (39) and (42) imply (19).

Acknowledgments

References

ANDERSON, T. and DARLING, D. (1952). Asymptotic theory of certain "goodness of fit" criteria based on stochastic processes. *Annals of Mathematical Statistics* **23** 193–212.

CARDOT, H., FERRATY, F., MAS, A. and SARDA, P. (2003a). Testing hypotheses in the functional linear model. *Scandinavian Journal of Statistics* **30** 241–255.

CARDOT, H., FERRATY, F. and SARDA, P. (2003b). Spline estimators for the functional linear model. *Statistica Sinica* **13** 571–591.

CUEVAS, A., FEBRERO, M. and FRAIMAN, R. (2002). Linear functional regression: the case of fixed design and functional response. *Canadian Journal of Statistics* **30** 285–300.

FERRATY, F., MAS, A. and VIEU, P. (2007). Nonparametric regression on functional data: inference and practical aspects. *Australian and New Zealand Journal of Statistics* **49** 459–461.

FERRATY, F. and VIEU, P. (2003). Curves discrimination: a nonparametric functional approach. *Computational Statistics & Data Analysis* **44** 161–173.

FERRATY, F. and VIEU, P. (2004). Nonparametric models for functional data, with application in regression, time-series prediction and curve discrimination. *Journal of Nonparametric Statistics* **16** 111–125. The International Conference on Recent Trends and Directions in Nonparametric Statistics.

FERRATY, F. and VIEU, P. (2006). *Nonparametric Functional Data Analysis.* Springer, New York, New York.

GASSER, T., HALL, P. and PRESNELL, B. (1998). Nonparametric estimation of the mode of a distribution of random curves. *Journal of the Royal Statistical Society: Series B (Statistical Methodology)* **60** 681–691.

GASSER, T., KÖHLER, W., MÜLLER, H.-G., KNEIP, A., LARGO, R., MOLINARI, L. and PRADER, A. (1984). Velocity and acceleration of height growth using kernel estimation. *Annals of Human Biology* **11** 397–411.

GAO, F., HANNIG, J. and TORCASO, F. (2003). Comparison theorems for small deviations of random series. *Electronic Journal of Probability* **8** 1–17.

GERVINI, D. and GASSER, T. (2005). Nonparametric maximum likelihood estimation of the structural mean of a sample of curves. *Biometrika* **92** 801–820.

HALL, P. and HECKMAN, N. E. (2002). Estimating and depicting the structure of a distribution of random functions. *Biometrika* **89** 145–158.

HALL, P. and HOROWITZ, J. L. (2007). Methodology and convergence rates for functional linear regression. *The Annals of Statistics* **35** 70–91.

JAMES, G. and SILVERMAN, B. (2005). Functional adaptive model estimation. *Journal of the American Statistical Association* **100** 565–576.

KNEIP, A. and GASSER, T. (1992). Statistical tools to analyze data representing a sample of curves. *Annals of Statistics* **20** 1266–1305.

RAMSAY, J. O. and DALZELL, C. J. (1991). Some tools for functional data analysis. *Journal of the Royal Statistical Society, Series B* **53** 539–572.

RAMSAY, J. O. and LI, X. (1998). Curve registration. *Journal of the Royal Statistical Society: Series B (Statistical Methodology)* **60** 351–363.

RAMSAY, J. O. and SILVERMAN, B. W. (2005). *Functional Data Analysis.* 2nd ed. Springer, New York.

RAO, C. R. (1958). Some statistical methods for comparison of growth curves. *Biometrics* **14** 1–17.

TUDDENHAM, R. and SNYDER, M. (1954). Physical growth of California boys and girls from birth to age 18. *Calif. Publ. Child Develop.* **1** 183–364.

YAO, F., MÜLLER, H.-G., CLIFFORD, A. J., DUEKER, S. R., FOLLETT, J., LIN, Y., BUCHHOLZ, B. A. and VOGEL, J. S. (2003). Shrinkage estimation for functional principal component scores with application to the population kinetics of plasma folate. *Biometrics* **59** 676–685.

YAO, F., MÜLLER, H.-G. and WANG, J.-L. (2005a). Functional data analysis for sparse longitudinal data. *Journal of American Statistical Association* **100** 577–590.

YAO, F., MÜLLER, H.-G. and WANG, J.-L. (2005b). Functional linear regression analysis for longitudinal data. *Annals of Statistics* **33** 2873–2903.
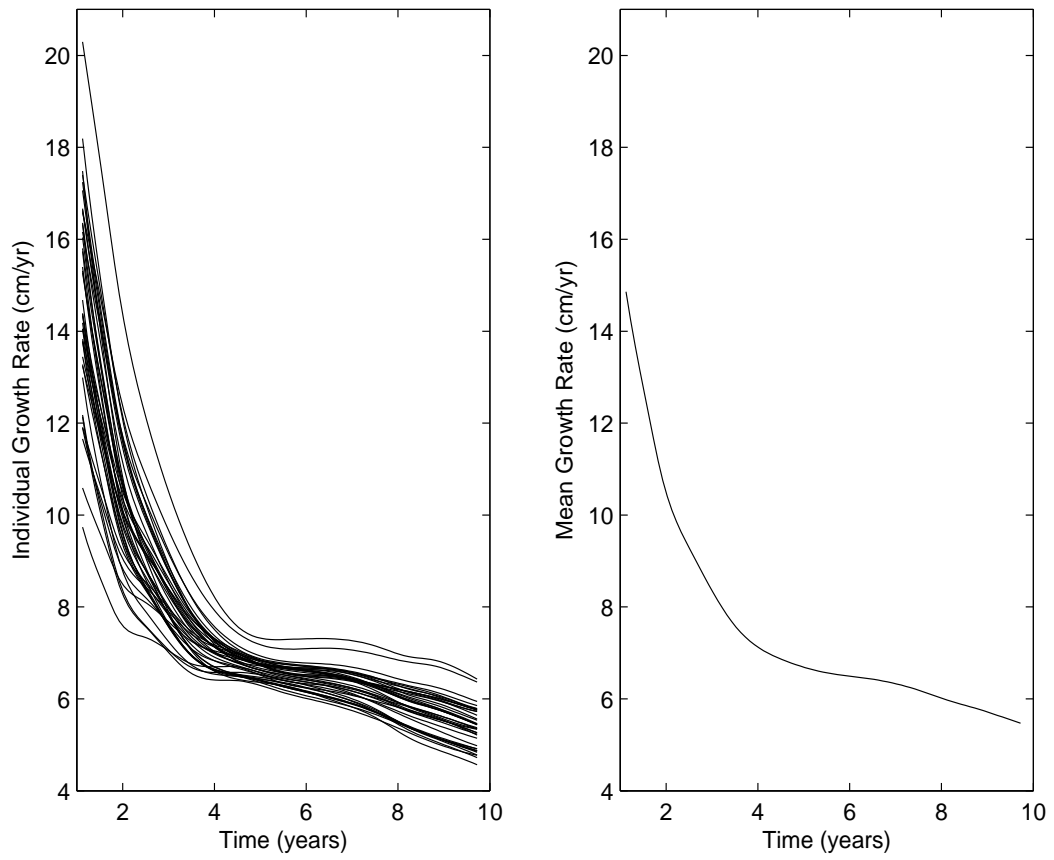
Figure 1: Fitted trajectories for individual predictor growth velocity curves (left panel) and mean growth velocity curve (right panel) for the Berkeley growth data ($n = 39$).
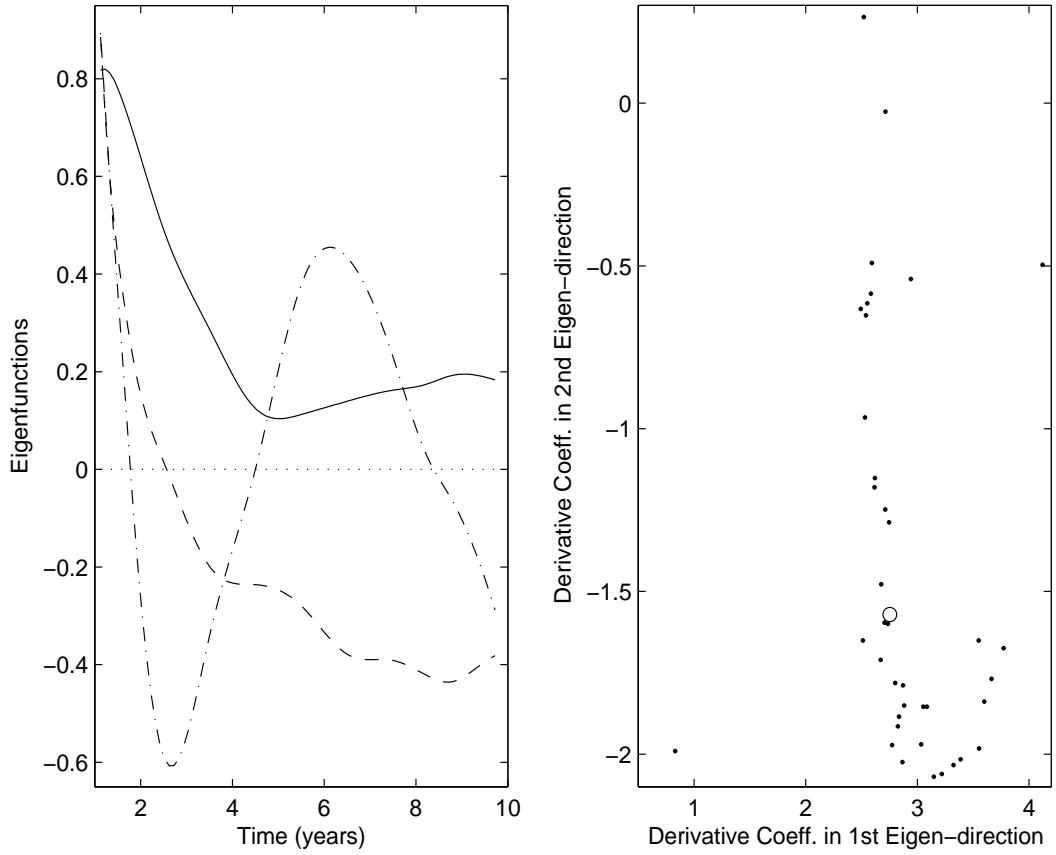
Figure 2: Smooth estimates of the first three eigenfunctions for the velocity growth curves, explaining 78.9% (solid), 17% (dashed) and 3.6% (dash-dotted) of the total variation, respectively (left panel) and estimated functional derivative coefficients $(\hat{\gamma}_{X_i,1}, \hat{\gamma}_{X_i,2})$ (7), in the directions of the first (x-axis) and second (y-axis) eigenfunction, evaluated at the predictor curves X_i (dots), as well as at the mean curve μ (circle) (right panel).
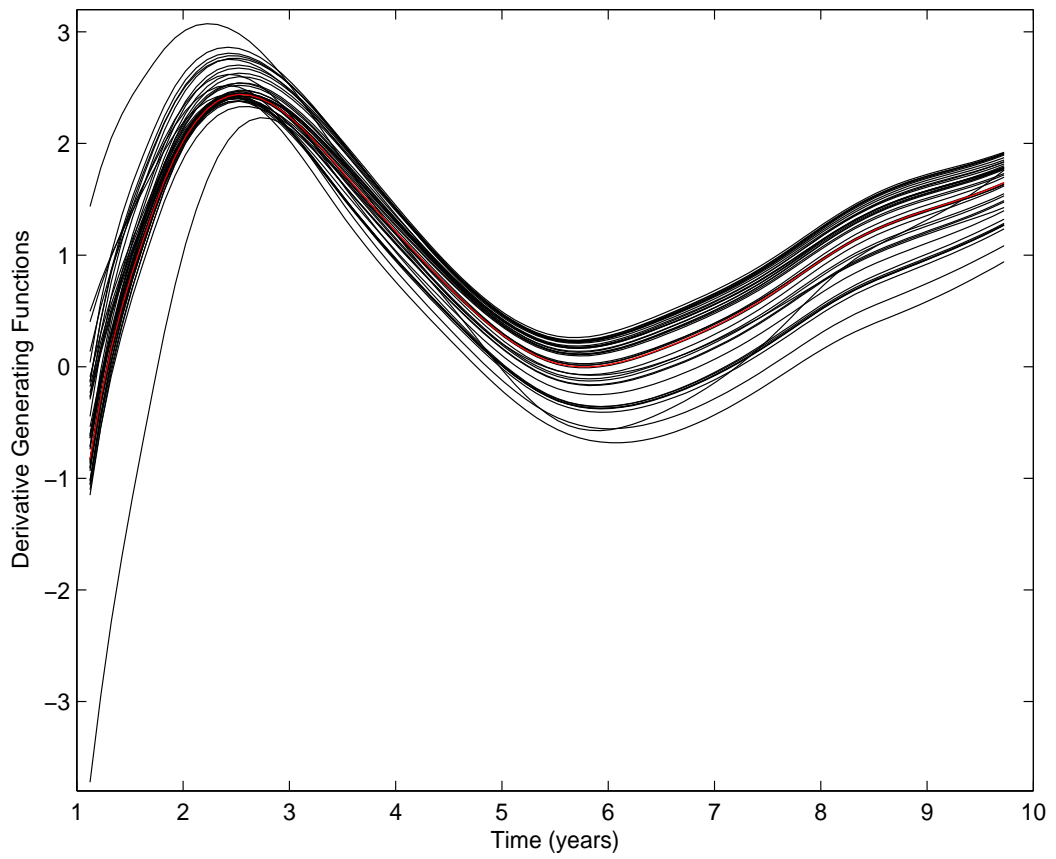
Figure 3: Estimated derivative generating functions $\hat{g}_i^*(t)$ (15) for all subjects X_i (black) and for the mean function (red) of the Berkeley growth data, based on the first three eigenfunctions.
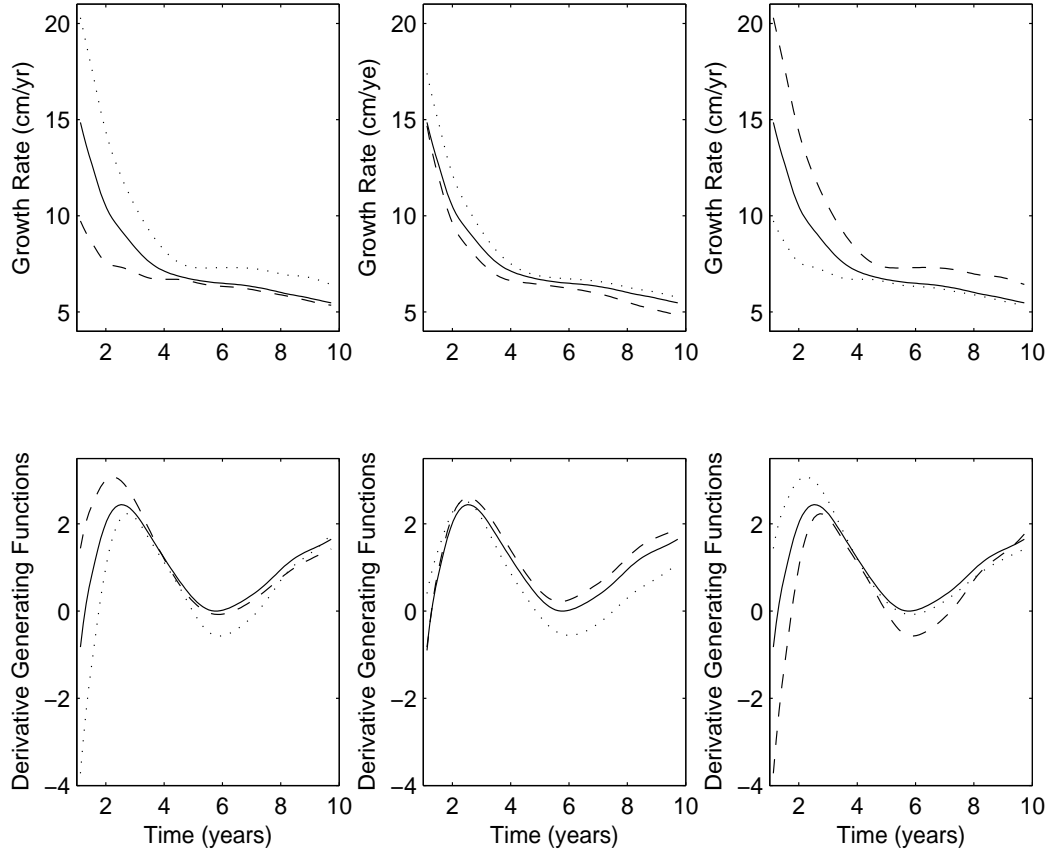
Figure 4: Predictor trajectories (top panels) and corresponding derivative generating functions $\hat{g}_i^*(t)$ (15) (bottom panels) which have the largest (dashed) and smallest (dotted) absolute values of derivative coefficients $\hat{\gamma}_{xj}$ (7) in the directions of the first ($j = 1$, left), second ($j = 2$, middle) and third ($j = 3$, right) eigenfunctions, as well as the mean functions (solid).
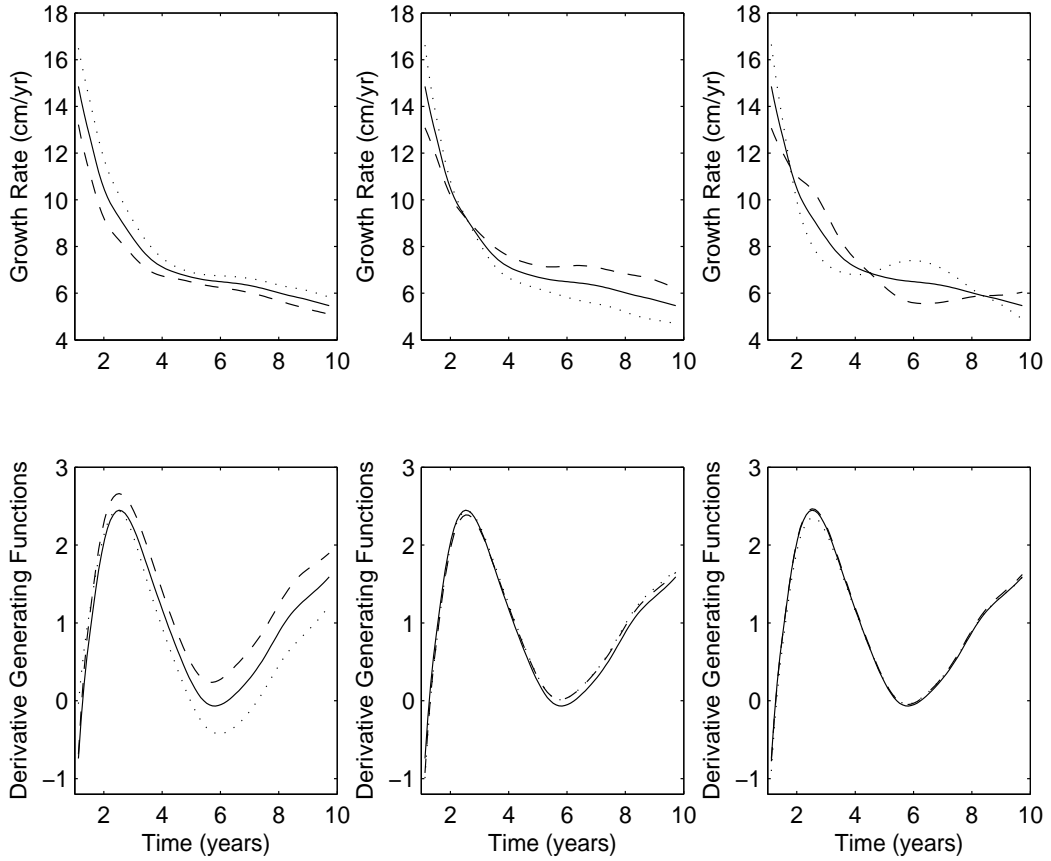
Figure 5: Top: Predictor trajectories $X(t; \alpha_j) = \hat{\mu}(t) + \alpha_j \hat{\psi}_j(t)$ with $\alpha_j = -2$ (dashed), 0 (solid), $+2$ (dotted), where $j = 1, 2, 3$ from left to right. Bottom: Corresponding derivative generating functions (15).